



**NAVAL
POSTGRADUATE
SCHOOL**

MONTEREY, CALIFORNIA

THESIS

**DETERMINING THE RELATIONSHIP BETWEEN
CUMULUS CLOUD WIDTH AND RADAR
REFLECTIVITY ECHO SIZE**

by

Aspen S. Bess

June 2021

Thesis Advisor:
Second Reader:

John M. Peters
Scott Powell

Approved for public release. Distribution is unlimited.

THIS PAGE INTENTIONALLY LEFT BLANK

REPORT DOCUMENTATION PAGE			<i>Form Approved OMB No. 0704-0188</i>
Public reporting burden for this collection of information is estimated to average 1 hour per response, including the time for reviewing instruction, searching existing data sources, gathering and maintaining the data needed, and completing and reviewing the collection of information. Send comments regarding this burden estimate or any other aspect of this collection of information, including suggestions for reducing this burden, to Washington headquarters Services, Directorate for Information Operations and Reports, 1215 Jefferson Davis Highway, Suite 1204, Arlington, VA 22202-4302, and to the Office of Management and Budget, Paperwork Reduction Project (0704-0188) Washington, DC, 20503.			
1. AGENCY USE ONLY (Leave blank)	2. REPORT DATE June 2021	3. REPORT TYPE AND DATES COVERED Master's thesis	
4. TITLE AND SUBTITLE DETERMINING THE RELATIONSHIP BETWEEN CUMULUS CLOUD WIDTH AND RADAR REFLECTIVITY ECHO SIZE			5. FUNDING NUMBERS
6. AUTHOR(S) Aspen S. Bess			
7. PERFORMING ORGANIZATION NAME(S) AND ADDRESS(ES) Naval Postgraduate School Monterey, CA 93943-5000			8. PERFORMING ORGANIZATION REPORT NUMBER
9. SPONSORING / MONITORING AGENCY NAME(S) AND ADDRESS(ES) N/A			10. SPONSORING / MONITORING AGENCY REPORT NUMBER
11. SUPPLEMENTARY NOTES The views expressed in this thesis are those of the author and do not reflect the official policy or position of the Department of Defense or the U.S. Government.			
12a. DISTRIBUTION / AVAILABILITY STATEMENT Approved for public release. Distribution is unlimited.			12b. DISTRIBUTION CODE A
13. ABSTRACT (maximum 200 words) The connection between updraft and downdraft size in cumulus clouds is an important part of weather prediction and thunderstorms. Understanding updraft width is important because of the connection between updraft width and entrainment. For instance, entrainment will have a greater negative effect on wider updrafts when compared to narrow updrafts. The larger the cloud width and updraft, the bigger the storm and potential impact. Yet updrafts are difficult to observe and measure from a single scanning radar because of variable beam angles relative to ascending air. Downdrafts, on the other hand, are readily observed by radar via the precipitation they contain because radar specifically detects the signal that is scattered back from precipitation particles. Therefore, with a consistent connection between updraft and downdraft width, radar measurements can provide better understanding of updraft attributes indirectly through observing downdrafts. In this study, the connection between updraft and downdraft width will be established through comparing updraft vertical velocities, downdraft radar reflectivity, and simulated radar attributes of cumulus clouds in a high-resolution numerical simulation.			
14. SUBJECT TERMS thunderstorms, weather prediction			15. NUMBER OF PAGES 39
			16. PRICE CODE
17. SECURITY CLASSIFICATION OF REPORT Unclassified	18. SECURITY CLASSIFICATION OF THIS PAGE Unclassified	19. SECURITY CLASSIFICATION OF ABSTRACT Unclassified	20. LIMITATION OF ABSTRACT UU

THIS PAGE INTENTIONALLY LEFT BLANK

Approved for public release. Distribution is unlimited.

**DETERMINING THE RELATIONSHIP BETWEEN CUMULUS CLOUD WIDTH
AND RADAR REFLECTIVITY ECHO SIZE**

Aspen S. Bess
Ensign, United States Navy
BS, U.S. Naval Academy, 2020

Submitted in partial fulfillment of the
requirements for the degree of

MASTER OF SCIENCE IN METEOROLOGY

from the

**NAVAL POSTGRADUATE SCHOOL
June 2021**

Approved by: John M. Peters
Advisor

Scott Powell
Second Reader

Wendell A. Nuss
Chair, Department of Meteorology

THIS PAGE INTENTIONALLY LEFT BLANK

ABSTRACT

The connection between updraft and downdraft size in cumulus clouds is an important part of weather prediction and thunderstorms. Understanding updraft width is important because of the connection between updraft width and entrainment. For instance, entrainment will have a greater negative effect on wider updrafts when compared to narrow updrafts. The larger the cloud width and updraft, the bigger the storm and potential impact. Yet updrafts are difficult to observe and measure from a single scanning radar because of variable beam angles relative to ascending air. Downdrafts, on the other hand, are readily observed by radar via the precipitation they contain because radar specifically detects the signal that is scattered back from precipitation particles. Therefore, with a consistent connection between updraft and downdraft width, radar measurements can provide better understanding of updraft attributes indirectly through observing downdrafts. In this study, the connection between updraft and downdraft width will be established through comparing updraft vertical velocities, downdraft radar reflectivity, and simulated radar attributes of cumulus clouds in a high-resolution numerical simulation.

THIS PAGE INTENTIONALLY LEFT BLANK

TABLE OF CONTENTS

I.	INTRODUCTION.....	1
	A. BACKGROUND	1
	B. MOTIVATION	1
	C. OBJECTIVES	2
II.	EXPERIMENT DESIGN	3
	A. MODEL SETUP.....	3
	1. 0-hour Model Profile.....	3
	2. 32-hour Model Simulation	5
	B. METHODS FOR ANALYZING LES RESULTS	6
	1. Threshold Values for w and R.....	6
	2. Histogram Percentiles and Time Series	7
III.	RESULTS	9
	A. HISTOGRAMS	9
	B. CORRELATION	10
	C. TIME SERIES.....	12
IV.	CONCLUSIONS	15
V.	FUTURE WORK.....	17
	LIST OF REFERENCES.....	19
	INITIAL DISTRIBUTION LIST	23

THIS PAGE INTENTIONALLY LEFT BLANK

LIST OF FIGURES

Figure 1.	Profiles of temperature and dewpoint were used to initialize the simulations, shown in a Skew-T log-P format. In red: temperature, (°C); green: dewpoint temperature (°C); thin red: virtual temperature (°C); black: the temperature an air parcel lifted adiabatically from the surface. Source: Peters et al. (2021).....5
Figure 2.	As in Figure 1, but showing the horizontally averaged properties of the simulation at 32 hours. Source: Peters et al. (2021).....6
Figure 3.	From left to right, area occupied by vertical velocity greater than 5 m s ⁻¹ , 10 m s ⁻¹ , and 15 m s ⁻¹ in km ²9
Figure 4.	From left to right, area occupied by reflectivity greater than 30 dBZ, 40 dBZ, and 50 dBZ in km ²10
Figure 5.	Correlation coefficients (CC, shading) between time series of each dBZ threshold and percentile (x-axis) and each <i>w</i> threshold and percentile (y-axis). Red shading indicates positive CC, and blue shading indicated negative CC.....11
Figure 6.	Time series on a time (hours) versus area (km ²) between <i>R</i> raw data at the 80 th percentile and 50 dBZ (light blue) and <i>w</i> raw data at the 90 th percentile and 10 m s ⁻¹ . Superimposed <i>R</i> data over 1 hour at the 80 th percentile and 50 dBZ (bold blue) and superimposed <i>w</i> data over 1 hour at the 90 th percentile and 10 m s ⁻¹ (bold red).12

THIS PAGE INTENTIONALLY LEFT BLANK

LIST OF ACRONYMS AND ABBREVIATIONS

AGL	above ground level
AMIE	atmospheric Madden-Julian Oscillation Investigation Experiment
ARM	atmospheric radiation measurement
CAPE	convective available potential energy
CIN	convective inhibition
CM1	Cloud Model 1
LES	large eddy simulations
R	radar reflectivity
w	vertical velocities

THIS PAGE INTENTIONALLY LEFT BLANK

ACKNOWLEDGMENTS

I would like to thank my thesis advisor, John Peters. Without his exceptional knowledge, guidance, and patience, this research would have not been possible. John Peters' consistent help with model simulations and coding were crucial for the success of this work and beneficial in my education in meteorology. I am extremely grateful for the devoted time and help, which was needed in order to make such progress.

I would like to express my gratitude to a few people from the meteorology program. I would like to thank Dr. Wendell Nuss for his guidance in choosing a helpful thesis advisor. I would like to thank Commander Ana Tempone for the initial start of the entire process and for facilitating the preponderance of my education. I would also like to thank Scott Powell and Qing Wang for thoughtful comments that improved the manuscript.

Finally, I would like to thank my family for their support during the countless hours put into this research. Their love has been unconditional during my career with the Navy and has been extremely beneficial to the success I have enjoyed here as a graduate student.

THIS PAGE INTENTIONALLY LEFT BLANK

I. INTRODUCTION

A. BACKGROUND

Strong updrafts in cumulonimbus clouds contribute to a wide range of severe weather hazards, including thunderstorms. Thunderstorms are important to understand because they produce even more hazardous weather like hail (Amburn and Wolf 1997), damaging winds (Brooks 2013), floods (Smith et al. 2001), tornadoes (Brooks 2013), and lightning (Marshall et al. 1995), which can impact daily life. Not only do they influence our daily lives, but also they are an integral part of our climate system as a major source of uncertainty in climate models (Brooks 2013). Stronger vertical velocities can equate to greater weather hazards and have a large influence on clouds in their surrounding environments (Giangrande et al. 2016). They are also able to more substantially redistribute heat and moisture vertically (Donner 1993). This influences synoptic and global-scale climate circulations (Price 2009).

Updraft vertical velocities (w) are primarily determined by buoyancy and pressure gradient accelerations (Peters et al. 2019). The two primary factors that influence buoyancy are convective available potential energy (CAPE) and entrainment (Zhang 2009). By far, the largest uncertainty in predicting storm characteristics from a given environment comes from predicting entrainment. Entrainment is also very difficult to measure in the field, and most studies of entrainment rely on large eddy simulations (LESs) rather than observations. In general, observational efforts to characterize entrainment rely on proxies, such as the degree of updraft dilution at a given height (Peters et al. 2020) and cloud top ascent rate (Gregory 2001). Another possible proxy that has been underused to date is updraft width. Theoretical studies and analyses of numerical simulations suggest that the width of updrafts is inversely correlated with their fractional entrainment rates (Peters et al. 2020). Thus, if we could measure updraft width, we would know a lot about entrainment.

B. MOTIVATION

Unfortunately, measuring updraft characteristics, including its width, in the real world is difficult, albeit less difficult than measuring entrainment. Such observation in

updraft characteristics require a vertically pointing radar that has a storm directly passing over in order to be perfectly observed (Battan et al. 1966) or a dual Doppler analysis that has limited area coverage and resolution (Oue et al. 2019). Dual Doppler analysis in particular requires two or more radars; they tend to have low resolution and are also inaccurate in the upper-troposphere.

Compared to updraft characteristics, precipitation is somewhat easy to measure via radar reflectivity. Furthermore, there is some evidence that downdraft size should correlate with updraft size (Moeng 2014). Since precipitation is connected to downdrafts, this means downdrafts may be more readily measurable than updrafts. By extension, this connection suggests that updraft area and precipitation area should be connected.

C. OBJECTIVES

There are other reasons that updraft area and precipitation area should be correlated. For example, greater vertical mass flux equates to greater precipitation production. Therefore, the main question is whether we can observe a precipitation area as a proxy for updrafts. The purpose of this project is to connect the updraft and downdraft using simulated radar reflectivity. The hypothesis is that if there is a large numerical outcome from both the precipitation area and vertical updraft, then a connection exists.

The organization of this thesis is as follows. Chapter II describes the setup for our numerical simulation, along with our methods for analyzing the simulation. Chapter III describes the results from this analysis. Finally, Chapters IV and V summarize the study, list the primary conclusions, and discuss the meaning of the results in the context of past and future work.

II. EXPERIMENT DESIGN

To address our objective, we ran a 36-hour-long LES of a thunderstorm environment. The goal of the analyses of the simulation was to correlate updraft and precipitation areas in the simulated results.

A. MODEL SETUP

This project uses a simulation of deep moist convection that was originally introduced by Peters et al. (2020). The simulation is run with Cloud Model 1 (CM1) version 19.10 (Bryan and Fritsch 2002). CM1 uses an acoustic time-splitting integration scheme (Durran and Klemp 1982), with a small time step used to integrate the equation terms that encapsulate acoustic dynamics, and the rest of the model prognostic variables integrated with a comparatively long-time step. Our long time step was set to 1 second. The vertical grid spacing was 50 m in the lowest 2 km that was linearly stretched to 250 m and then held constant at 250 m up to the top of the model at 20 km (Peters 2020). Similar to the setup in Peters et al. (2020), the grid spacing horizontally was set at 0.1 km, and the east and west domain lengths were both 64 km, with periodic boundary conditions. Initial and lateral boundaries were periodic, with a constant enthalpy flux from the ocean and a semi-slip lower boundary, and a free-slip upper boundary. Turbulence also plays a factor in entrainment in deep convection. Temperature perturbations with an amplitude of 0.25 K were included in the initial conditions to facilitate the development of turbulence, as was done in Peters et al. (2020). The simulation then ran for 36 hours. We parameterized microphysics by applying the double moment scheme of Morrison et al. (2009) with hail mixing ratios and number concentrations explicitly predicted. The first 20 hours displayed shallow- to-mid-level convection with maximum cloud top below 10 km (Peters et al. 2020). Beyond 20 hours, bursts of deep convection occurred with less active periods.

1. 0-hour Model Profile

Peters et al. (2020) uses Yoneyama’s 2013 Atmospheric Radiation Measurement (ARM) Madden-Julian Oscillation Investigation experiment, which derives a sounding from a tropical environment using rawinsonde data and was post-processed and quality

controlled by Ciesielski (2014). The sounding is shown in Figure 1. This project was modeled after Peters et al. (2020) in order to further investigate connections between updrafts and radar reflectivity. The parameters used, as in Peters et al. (2020), were mean values of temperature and horizontal wind profiles obtained during the time period of 1 October 2011—15 January 2012. To compute the mass fraction of water vapor, we use the mean value it was observed during rainy days from radiosonde launches during the same time period within 150 km radius of the launch site (Peters et al. 2020). The surface pressure and water vapor were also collected during the rainy periods and the surface temperature was the mean value across all soundings during this time period (Peters et al. 2020) in order to give the most accurate model that relays a real-time dynamic atmosphere.

The skew T -log p diagram represents an air parcel that was lifted adiabatically as shown in the black line. The red line displays the temperature ($^{\circ}\text{C}$), the green line displays dewpoint temperature ($^{\circ}\text{C}$), and the thin red line represent virtual temperature ($^{\circ}\text{C}$). Overall, this environment shows a convectively unstable atmosphere. There is moderate CAPE around $\sim 2000 \text{ J kg}^{-1}$ and small convective inhibition (CIN), with a relatively moist free troposphere.

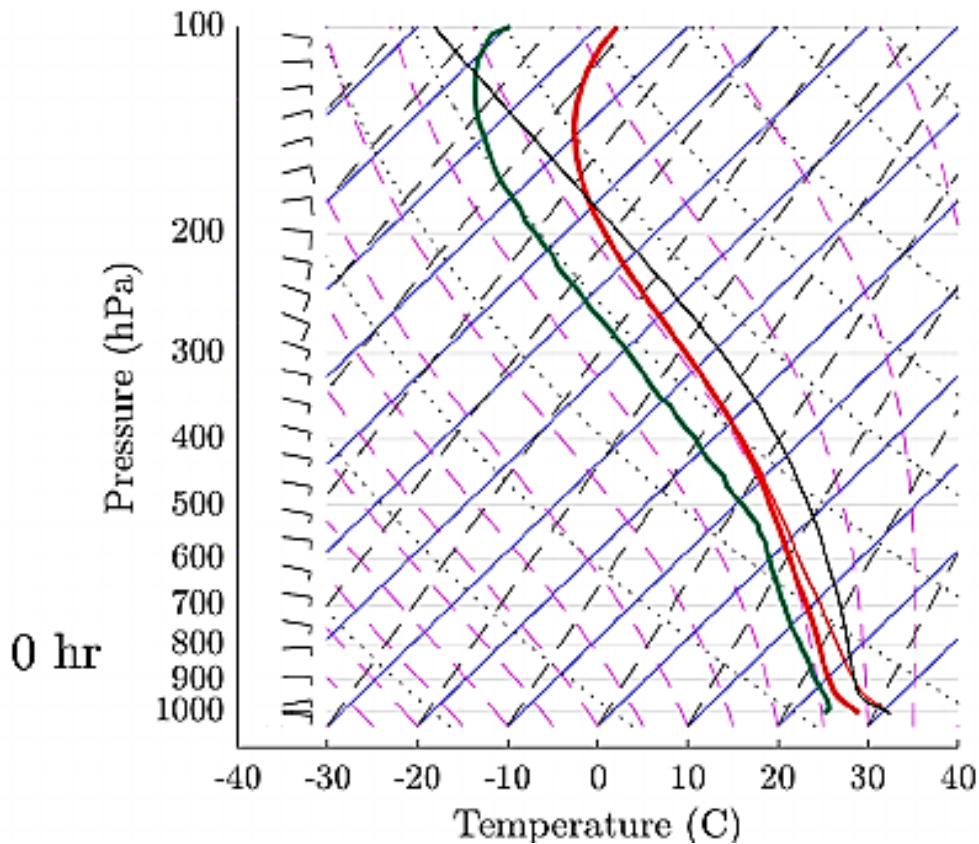


Figure 1. Profiles of temperature and dewpoint were used to initialize the simulations, shown in a Skew-T log-P format. In red: temperature, ($^{\circ}\text{C}$); green: dewpoint temperature ($^{\circ}\text{C}$); thin red: virtual temperature ($^{\circ}\text{C}$); black: the temperature an air parcel lifted adiabatically from the surface. Source: Peters et al. (2021).

2. 32-hour Model Simulation

This simulation was run for a total of 36 hours showing the 32-hour profile depicted in Figure 2. The same initial process was used in Figure 1 as well as the same represented in the skew T -log p diagram. This environment displays a similar profile as Figure 1, but slightly warmer air near the surface. There is also an increase in CAPE to $\sim 3000 \text{ J kg}^{-1}$.

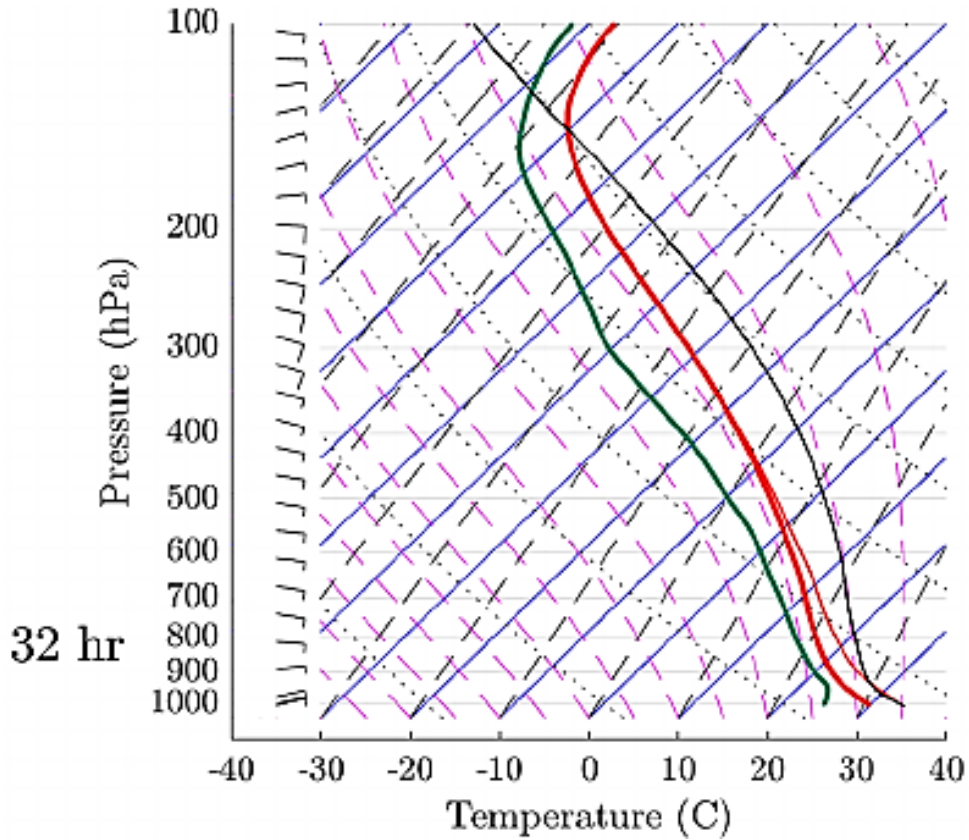


Figure 2. As in Figure 1, but showing the horizontally averaged properties of the simulation at 32 hours. Source: Peters et al. (2021).

B. METHODS FOR ANALYZING LES RESULTS

1. Threshold Values for w and R

At each time in the simulation, we computed a 2-dimensional map of the column maximum vertical velocity, w , at each grid point, along with a 2-dimensional map of S-band radar reflectivity factor, R , at 1 km above ground level (AGL). We then identified continuous regions within these w and R fields that exceeded threshold values. The thresholds used for w were greater than 1, 5, 10, 15 and 20 m s^{-1} . The thresholds used for R were greater than 30, 40 and 50 dBZ.

2. Histogram Percentiles and Time Series

Once these continuous regions were established, we calculated the areas of each one. At each time, histograms of the areas of continuous w and R were created for each threshold. From the histogram, the 50th, 60th, 70th, 80th, and 90th percentiles of w and R were computed. This resulted in the times series of percentiles of w and R . Lastly, correlations between the two time series were computed. To validate the primary hypothesis of the thesis, we looked for statistically significant positive linear correlations between the time series of w percentiles, and the time series of R percentiles. Statistical significance was determined using a 95% confidence level, which was obtained via a Student's t-test, assuming that both variables were normally distributed. All the discussed correlation coefficients were tested to be statistically significant, unless stated otherwise.

THIS PAGE INTENTIONALLY LEFT BLANK

III. RESULTS

A. HISTOGRAMS

In Figure 3, histograms were created for continuous areas of vertical velocity larger than 5, 10, and 15 m s⁻¹. These histograms show a large number of small w areas and fewer large ones. This result is consistent with previous studies by Neggers et al. (2019) and Peters et al. (2020), which have shown that the distribution of cloud sizes tends to be inverse exponential with respect to updraft width.

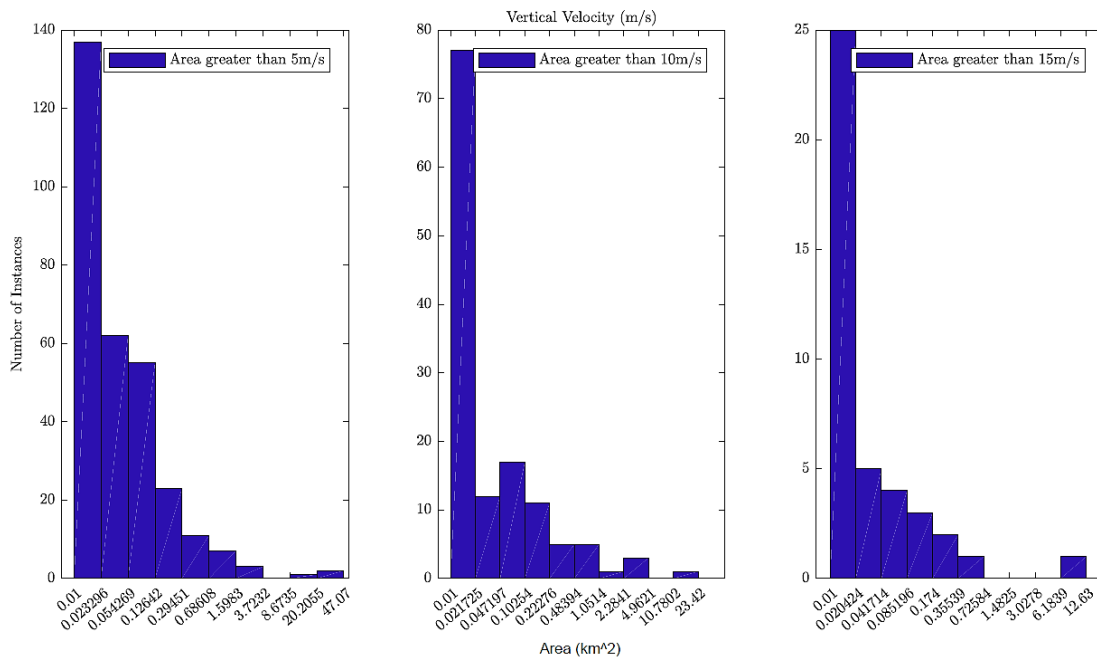


Figure 3. From left to right, area occupied by vertical velocity greater than 5 m s⁻¹, 10 m s⁻¹, and 15 m s⁻¹ in km².

In Figure 4, histograms were created for continuous areas of reflectivity greater than 30, 40, and 50 dBZ. These also display large numbers of small R continuous areas with few large area coverages. The general shape is similar to that of vertical velocity and has decreasing numbers as the area increases. At face value, these trends point to a possible connection between w and R that is explored further later.

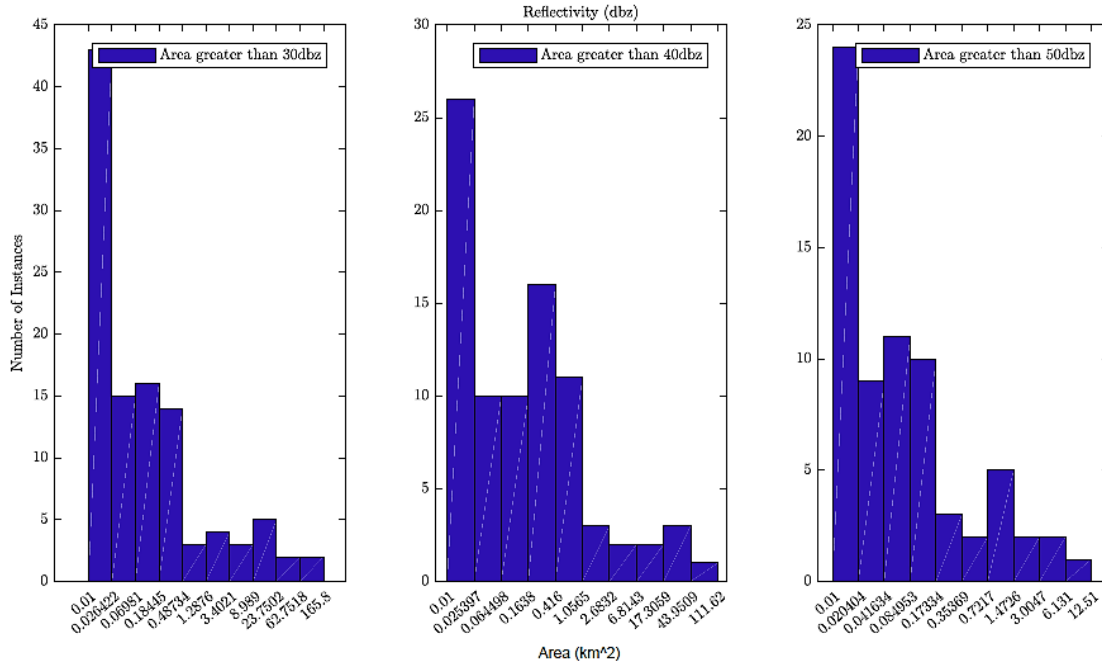


Figure 4. From left to right, area occupied by reflectivity greater than 30 dBZ, 40 dBZ, and 50 dBZ in km^2 .

B. CORRELATION

The goal of the correlation in Figure 5 was to match an attribute from the R , on the x-axis, to an attribute from the w on the y-axis. The shading shows the correlation. When there is red, there is a positive correlation. When there is blue, there is a negative correlation. Overall, the correlations varied throughout. However, the maximum values were on the order of ± 0.5 , which is considered a “moderate” correlation.

Figure 5 also displays a magenta ‘x’ where the best correlation is located at the 90th percentile for 20 m s^{-1} in w and the 80th percentile for 50 dBZ in R . In order to visualize these time series, they are plotted against each other in Figure 6.

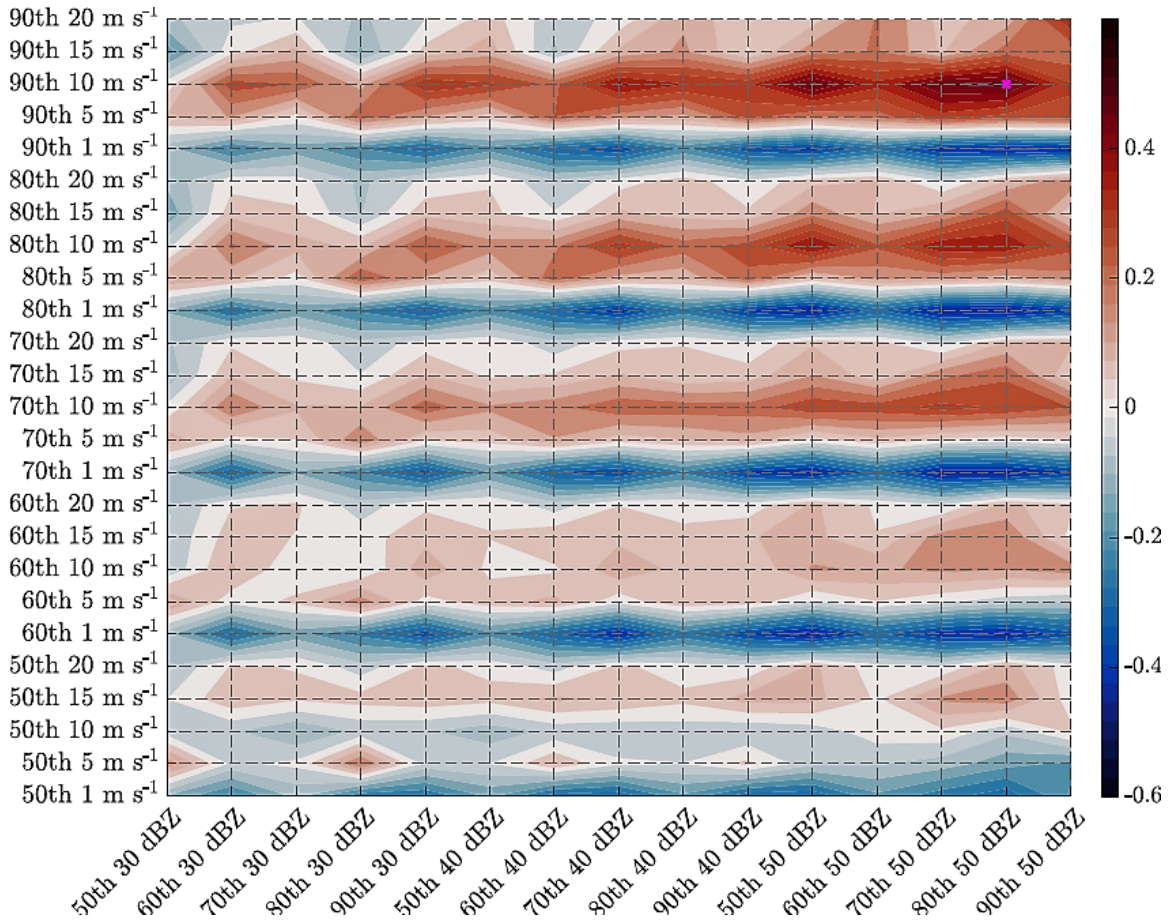


Figure 5. Correlation coefficients (CC, shading) between time series of each dBZ threshold and percentile (x-axis) and each w threshold and percentile (y-axis). Red shading indicates positive CC, and blue shading indicated negative CC.

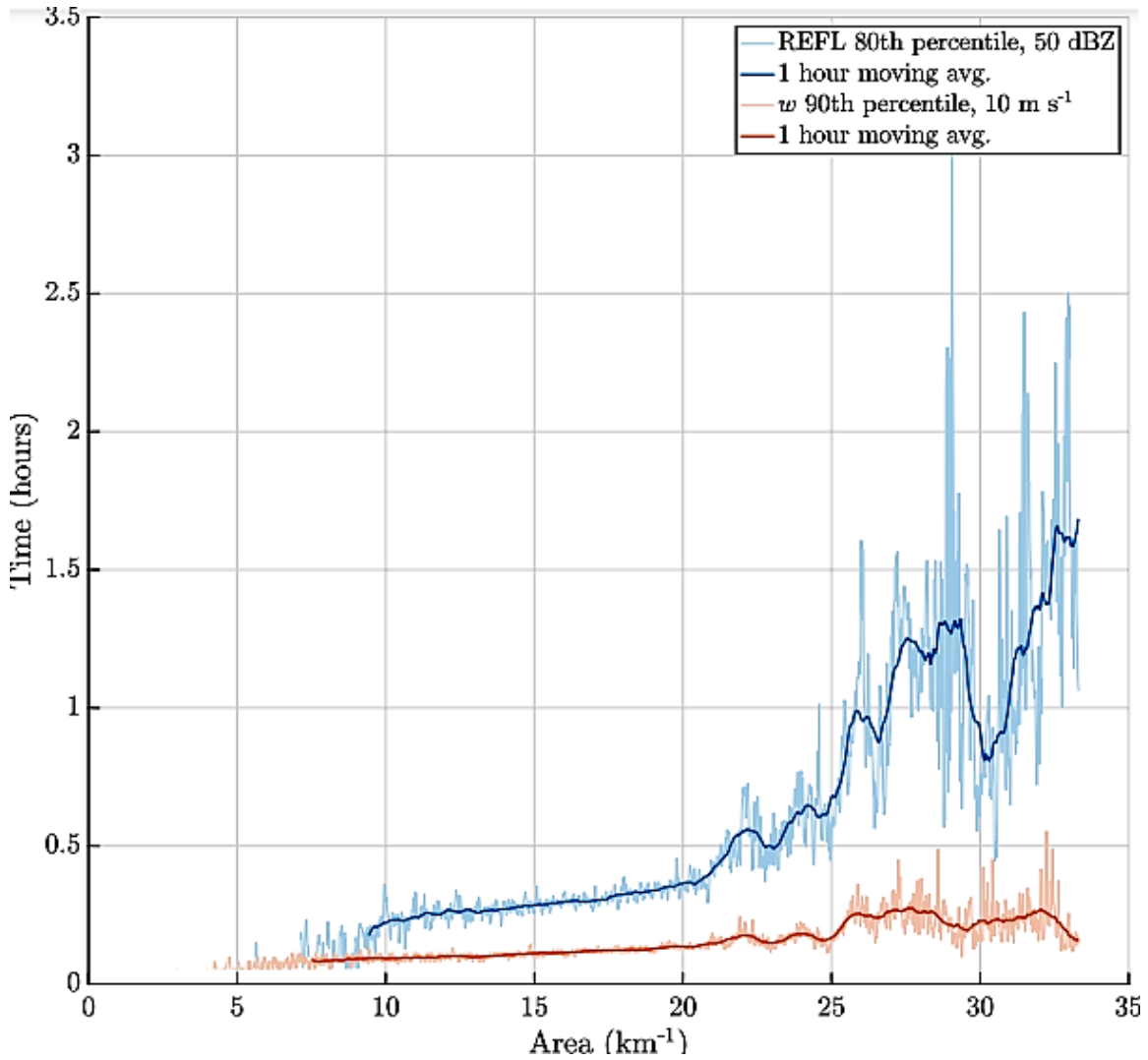


Figure 6. Time series on a time (hours) versus area (km^2) between R raw data at the 80th percentile and 50 dBZ (light blue) and w raw data at the 90th percentile and 10 m s^{-1} . Superimposed R data over 1 hour at the 80th percentile and 50 dBZ (bold blue) and superimposed w data over 1 hour at the 90th percentile and 10 m s^{-1} (bold red).

C. TIME SERIES

Overall, a moderate correlation can be observed in Figure 6. The bold blue and bold red line represent superimposed data averaged over 1 hour to display less noise within each time series. During the first 22 hours, both w and R show similar variation to one another, having peaks and minima at similar times. This is representative of the simulated shallow convection. After 22 hours, the shallow convection transitions to deep convection. When

following the time series, there are several similarities among the w and R during deep convection. Around 23 hours, both demonstrate an increase in area as well as around 24 hours. At 25 hours, they display a decrease in area at the same time, and so on and so forth until the end. The only time they do not perfectly align is right at the end. The R shows an increase while the w shows a decrease of area over time. Although the correlation does not display the exact same area per variable, it does demonstrate a similar trend.

THIS PAGE INTENTIONALLY LEFT BLANK

IV. CONCLUSIONS

Thunderstorms play an important role in both weather and climate. Accurate weather and climate forecasts require that numerical weather prediction and climate models correctly represent the effects of thunderstorms. In this thesis, we have investigated the potential connection between the size of thunderstorm updrafts, and the size of their areas of observable simulated radar reflectivity. We investigated this connection to see if reflectivity areas, which is relatively easily measurable using radar observations, can be used as a proxy for observing updraft area, which is comparatively difficult to directly observe.

Our conclusions are as follows:

- In a large eddy simulation, updraft areas are moderately correlated with reflectivity areas when certain specific thresholds for defining updraft and reflectivity area are used.
- The maximum correlation coefficient between updraft area and reflectivity area was approximately 0.5. This maximum correlation occurred when updrafts were defined as regions of maximum column vertical velocity greater than 10 m s^{-1} , and simulated composite reflectivity greater than 50 dBZ.

This work is significant because radar measurements of refractivity from field campaigns can be used to infer updraft characteristics. With these characteristics, possible connections can be made to environmental qualities such as wind shear, CAPE, CIN, vorticity, and updraft area. In addition, forecasters can use this as a proxy for updraft size and strength in convective events.

THIS PAGE INTENTIONALLY LEFT BLANK

V. FUTURE WORK

A moderate correlation between w area and R area was found, however, there is still work that needs to be done. Since comparing distributions were made, it would be of more interest and beneficial to match the w areas with the R areas in a more robust manner. Future work should also look at simulations and observations over a range of different environments since only one environment was used in the simulation here. Additionally, observations of non-precipitating shallow convection using precipitation radar do not capture the downdrafts of many clouds. The downdraft and updraft characteristics of these clouds should be observed using higher-frequency cloud radar such as scanning Ka-band radars in order to conduct a similar analysis.

THIS PAGE INTENTIONALLY LEFT BLANK

LIST OF REFERENCES

- Amburn, S.A., and Wolf, P.L., 1997: VIL density as a hail indicator, *Weather and Forecasting*, **12**, 473–478, [https://doi.org/10.1175/1520-0434\(1997\)012<0473:VDAAHI>2.0.CO;2](https://doi.org/10.1175/1520-0434(1997)012<0473:VDAAHI>2.0.CO;2).
- Batan, L.J., and Theiss, J.B., 1966: Observations of vertical motions and particle sizes in a thunderstorm, *Journal of the Atmospheric Sciences*, **23**, 78–87, [https://doi.org/10.1175/1520-0469\(1966\)023<0078:OOVMAP>2.0.CO;2](https://doi.org/10.1175/1520-0469(1966)023<0078:OOVMAP>2.0.CO;2).
- Brooks, H.E., 2013: Severe thunderstorms and climate change, *Atmospheric Research*, **123**, 129–138, <https://doi.org/10.1016/j.atmosres.2012.04.002>.
- Bryan, G.H., and Fritsch, J.M., 2002: A benchmark simulation for moist nonhydrostatic numerical models, *Monthly Weather Review*, **130**, 2917–2928, [https://doi.org/10.1175/1520-0493\(2002\)130<2917:ABSFMN>2.0.CO;2](https://doi.org/10.1175/1520-0493(2002)130<2917:ABSFMN>2.0.CO;2).
- Ciesielski, P.E., Yu, H., Johnson, R.H., Yoneyama, K., Katsumata, M., Long, C.N., Wang, J., Loehrer, S.M., Young, K., Williams, S.F., Brown, W., Braun, J., and Van Hove, T., 2014: Quality-controlled upper-air sounding dataset for DYNAMO/CINDY/AMIE: Development and corrections, *Journal of Atmospheric and Oceanic Technology*, **31**, 741–764, <https://doi.org/10.1175/JTECH-D-13-00165.1>.
- Donner, L.J., 1993: A cumulus parameterization including mass fluxes, vertical momentum dynamics, and mesoscale effects, *Journal of Atmospheric Sciences*, **50**, 889–906, [https://doi.org/10.1175/1520-0469\(1993\)050<0889:ACPIMF>2.0.CO;2](https://doi.org/10.1175/1520-0469(1993)050<0889:ACPIMF>2.0.CO;2).
- Durrant, D.R., and Klemp, J.B., 1982: On effects of moisture on the Brunt-Vaisala frequency, *Journal of the Atmospheric Sciences*, **39**, 2152–2158, [https://doi.org/10.1175/1520-0469\(1982\)039<2152:OTEOMO>2.0.CO;2](https://doi.org/10.1175/1520-0469(1982)039<2152:OTEOMO>2.0.CO;2).
- Giagrande, S.E., Toto, T., Jensen, M.P., Bartholomew, M.J., Feng, Z., Protat, A., Williams, C.R., Schumacher, C., and Machado, L., 2016: Convective cloud vertical velocity and mass-flux characteristics from radar wind profiler observations during GoAmazon2014/5, *Journal of Geophysical Research Atmospheres*, **121**, 12,891–12,913, <https://doi.org/10.1002/2016JD025303>.
- Gregory, D., 2001: Estimation of entrainment rate in simple models of convective clouds, *Quarterly Journal of the Royal Meteorological Society*, **127**, <https://doi.org/10.1002/qj.49712757104>.

- Marshall, T.C., McCarthy, M.P., and Rust, W.D., 1995: Electric field magnitudes and lightning initiation in thunderstorms, *Journal of Geophysical Research Atmospheres*, **100**, 7097–7103, <https://doi.org/10.1029/95JD00020>.
- Moeng, C.H., 2014: A closure for updraft-downdraft representation of subgrid-scale fluxes in cloud-resolving models, *Monthly Weather Review*, **142**, 703–715, <https://doi.org/10.1175/MWR-D-13-00166.1>.
- Morrison, H., Thompson, G., and Tatarskii, V., 2009: Impact of cloud microphysics on the development of trailing stratiform precipitation in a simulated squall line: Comparison of One- and Two-Moment Schemes, *Monthly Weather Review*, **137**, 991–1007, <https://doi.org/10.1175/2008MWR2556.1>.
- Neggers, R.A., Griewank, P.J., and Heus, T., 2019: Power-law scaling in the internal variability of cumulus cloud size distributions due to subsampling and spatial organization. *Journal of the Atmospheric Sciences*, **76**, 1489–1503, <https://doi.org/10.1175/JAS-D-18-0194.1>.
- Oue, M., Kollias, P., Shapiro, A., Tatarevic, A., and Matsui, T., 2019: Investigation of observational error sources in multi-Doppler-radar three-dimensional variational vertical air motion retrievals, *Atmospheric Measurement Techniques*, **12**, 1999–2018, <https://doi.org/10.5194/amt-12-1999-2019>.
- Peters, J.M., Morrison, H., Varble, A.C., Hannah, W.M., Gianrande, S.E., 2020: Thermal chains and entrainment in cumulus updrafts. part I: Theoretical description, *Journal of the Atmospheric Sciences*, **77**, 3637–3660, <https://doi.org/10.1175/JAS-D-19-0243.1>.
- Peters, J.M., Morrison, H., Zhang, G.J., and Powell, S.W., 2020: Improving the physical basis for updraft dynamics in deep convection parameterizations, *Journal of Advances in Modeling Earth Systems*, **13**, <https://doi.org/10.1029/2020MS002282>.
- Peters, J.M., Nowotarski, C.J., and Morrison, H., 2019: The role of vertical wind shear in modulating maximum supercell updraft velocities, *Journal of the Atmospheric Sciences*, **76**, <https://doi.org/10.1175/JAS-D-19-0096.1>.
- Price, C., 2009: Thunderstorms, lightning, and climate change, *Lightning: Principles, Instruments and Applications*, 521–535, https://doi.org/10.1007/978-1-4020-9079-0_24.
- Smith, J.A., Baeck, M.L., Zhang, Y., and Doswell III, C.A., 2001: Extreme rainfall and flooding from supercell thunderstorms, *Journal of Hydrometeorology*, **2**, 469–489, [https://doi.org/10.1175/1525-7541\(2001\)002<0469:ERAFFS>2.0.CO;2](https://doi.org/10.1175/1525-7541(2001)002<0469:ERAFFS>2.0.CO;2).

Yoneyama, K., Zhang, C., and Long, C.N., 2013: Tracking pulses of the Madden-Julian Oscillation, *Bulletin of the American Meteorological Society*, **94**, 1871–1891, <https://doi.org/10.1175/BAMS-D-12-00157.1>.

Zhang, G.J., 2009: Effects of entrainment on convective available potential energy and closure assumptions in convection parameterization, *Journal of Geophysical Research Atmospheres*, **114**, <https://doi.org/10.1029/2008JD010976>.

THIS PAGE INTENTIONALLY LEFT BLANK

INITIAL DISTRIBUTION LIST

1. Defense Technical Information Center
Ft. Belvoir, Virginia
2. Dudley Knox Library
Naval Postgraduate School
Monterey, California